Characteristics of Seismic Source Spectra from the Chia-Yi and Tai-Nan area of Taiwan

Win-Gee Huang[1,2] and Yeong Tein Yeh[1]

ABSTRACT

Source spectra of S waves were determined using records of eighteen earthquakes occurring in the Chia-Yi and Tai-Nan area with local magnitudes of $2.8 \leq M_L \leq 5.8$ as obtained from a rock-site station. In addition to the correction of geometrical spreading, elimination of the anelastic attenuation effect from the observed spectra was carefully examined to measure the high-frequency spectral levels of seismic sources.

As to the source spectra, two types of spectral shapes may be observed. For earthquakes of $M_L < 5.4$, the spectra obey the ω-squared model with a single corner frequency. However, this observation cannot provide an adequate representation for earthquakes of $M_L \geq 5.4$, since they clearly demonstrate the existence of two corner frequencies on the spectrum. The difference in spectral shapes may reveal that the rupture of larger earthquakes proceeded as a series of multiple events while a single fault patch results in smaller earthquakes. This explanation is supported by both spectral shapes and waveform characteristics, and may disclose the complexity of earthquake sources of larger magnitude.

The seismic moment of M_0 measured from spectral level at low frequency range satisfies a relation with lower corner frequency of f_0 in $M_0 \propto f_0^{-3}$. For the set of earthquakes, the average stress drop is 125 bars. Nonetheless, this model is a poor fit to the shapes of source spectra for events of $M_L \geq 5.4$. The source spectra obtained by the two greater events, the 1991 Chiali ($M_L = 5.7$) and 1993 Tapu ($M_L = 5.8$) earthquakes, were discussed in this subject. In describing these spectra, a stress drop of about 60 bars was estimated from the spectral level in a lower frequency range, while 600 bars was required to interpret the high-frequency amplitudes. By applying the Sato and Hirasawa (1973) source model, the average scale length of the fault heterogeneities inferred from the higher corner frequency of f_0 is about 300 meters, and this is almost identical to the source radius of the Brune (1970, 1971) model for small events with a magnitude of around 3. Based on the seismic moments taken from the Harvard centroid-mo-

---

[1]Institute of Earth Sciences, Academia Sinica, P.O. Box 1-55, Nankang, Taipei, Taiwan, ROC
[2]Institute of Geophysics, National Central University, Chungli, Taoyuan, Taiwan, ROC

ment tensor (CMT) solution and this study, for the Tapu earthquake the estimated values of local stress drop obtained using the specific barrier model (Papageorgiou and Aki, 1983) are about 700 and 516 bars. The high stress drop of 600 bars for our result, as observed from high-frequency source spectra, lies in between, and its validity is also confirmed by the agreement of total seismic energy between the results obtained from specific barrier model and those from the Gutenberg-Richter relation (1956).

(Key words: Anelastic attenuation, Corner frequency, Seismic moment, Stress drop, Specific barrier model)

1. INTRODUCTION

The Chia-Yi and Tai-Nan (hereafter referred to as CN) plain is one of the most seismically active areas on Taiwan island. According to historical records, several disastrous earthquakes occurred in this area since 1700 (Cheng and Yeh, 1989). As discussed by Cheng and Yeh (1985), the average rate of damaging earthquakes with $M_L > 6$ occurring in the region is approximately in every 25 years. No major event has occurred in this area since the 1964 Paiho earthquake ($M_L = 6.4$). Although future large and catastrophic earthquakes are anticipated in this region, predictions of strong-ground motion in this area are hindered by a lack of data for large events. For this reason, a number of film-recording accelerographs have been operated by the Institute of Earth Sciences (IES) in the CN area since 1972. Unfortunately, most of the stations are placed in the basement of civil structures and in buildings. In order to obtain the free-field ground motions generated by earthquakes, National Chung-Cheng University (NCCU) installed a local digital accelerographic network with fourteen stations in the CN area and this began operating in 1990. Even with these improvements, there are still too few to attain a high probability of recording strong motion information for earthquakes. Thus, if we want to extract the source parameters from them, extensive sets of near-source ground-motion recordings are desirable. Later, in 1993, a new digital dense array of strong-motion seismographs, consisting of more than one-hundred stations, was widely deployed in this area by the Central Weather Bureau (CWB). Since then, the ground motion database for southwestern Taiwan has improved greatly.

During the past few years, many earthquakes of small-to-moderate magnitude have been located in the CN area. Because the strong motion stations are densely distributed, these earthquakes produced many near-source ground-motion records. At near-source distances, these recordings are dominated by primary S waves. These phases are important both for their direct association with the strongest ground motions of engineering interest, as well as for their frequency content which is of direct relevance to the distribution of heterogeneities of the fault plane. Results from previous ground-motion predictions in a close-in sites (e.g., Brune, 1970; Hanks and McGuire, 1981; Aki, 1979; Pagageorgiou and Aki 1983; Boatwright, 1988) led one to believe that the interaction of the rupture front with the heterogeneities over the fault plane is responsible for the radiation of high-frequency waves. Traditionally, such a description can

be in terms of the S-wave source spectrum (accounting properly for attenuation and site amplification) and its associated high-frequency spectral content of the radiated waves. The high-frequency excitation of earthquake sources has attracted the attenuation not only because it might be used to improve our understanding of the character of quasi-static and dynamic stress differences during the faulting, but also because it can be used to account for the heterogeneities of slip distribution on a fault plane.

Only a few studies have been done on information concerning earthquake source spectra in the CN area. Based on the theoretical model from Brune (1970, 1971), Ou and Tsai (1993) and Tsai (1997) constructed the scaling of the earthquake sources from the relation of seismic moments and corner frequencies of source S-wave spectra. Using the dataset from locally recorded earthquakes from 1976 to 1992, Ou and Tsai (1993) showed that the seismic moments are proportional to the corner frequencies in a power law with an exponent value of -3. They concluded that Brune's model, with an average stress drop of about 150 bars, can adequately represent the source spectra for earthquakes $3.6 \leq M_L \leq 6.3$. In a substantial analysis using data from 1990 to 1993, Tsai (1997) did not support the above conclusion as a general feature of CN earthquakes with $M_L \geq 4$. He reported that the seismic moment does not scale with corner frequency in a commonly used power law with an exponent value of -3. This suggests a breakdown in constant stress drop scaling. Tsai (1997) stressed that this controversy may be due to insufficient strong-motion data to adequately judge the relation from his study. The apparent discrepancy of the scaling behavior of earthquake source from the above two studies may arise from different instruments and from different recordings. The data used by Ou and Tsai (1993) included some of the events from old instruments (pre-1990), and there has been concern about uncertain instrument calibration (Wang, 1988). Furthermore, the correction for attenuation and geometrical spreading possibly biased both studies because the recordings are from a variety of sites. Also, in consideration of the different seismic circumstances, the earthquakes used by Ou and Tsai (1993) were located in a region confined by 23°-24°N and 120°-121°E; however, Tsai (1997) considered the events within an area bound by 21°-23.5°N and 119°-121°E. Thus, source parameters obtained by Tsai (1997) might only be the average values for the whole of southwestern Taiwan and cannot be reasonably representative of a particular area, e.g., the CN area. Consequently, one question that may be posed but not yet answered is: what is the scaling law of small to moderate earthquakes which is applicable in the CN area?

The work of this article is to estimate source parameters based on modeling source spectra of S-waves. First, we inspect the anelastic attenuation (Q) model currently used in the CN area to remove its effects from the observed spectra. Next, source parameters, i.e., source dimension, stress drop and seismic moment of the earthquakes are estimated through the spectrum-fitting technique developed by Brune (1970). Our goal is to understand the source characteristics for small to moderate earthquakes. In this paper, we report the results of our study on source spectra.

2. A NEW DATA-SET OF STRONG-GROUND MOTIONS

The CN strong-motion network is operated jointly by the CWB and NCCU. Figure 1 shows the layout of the free-field stations and the mapped fault traces near the network. Each
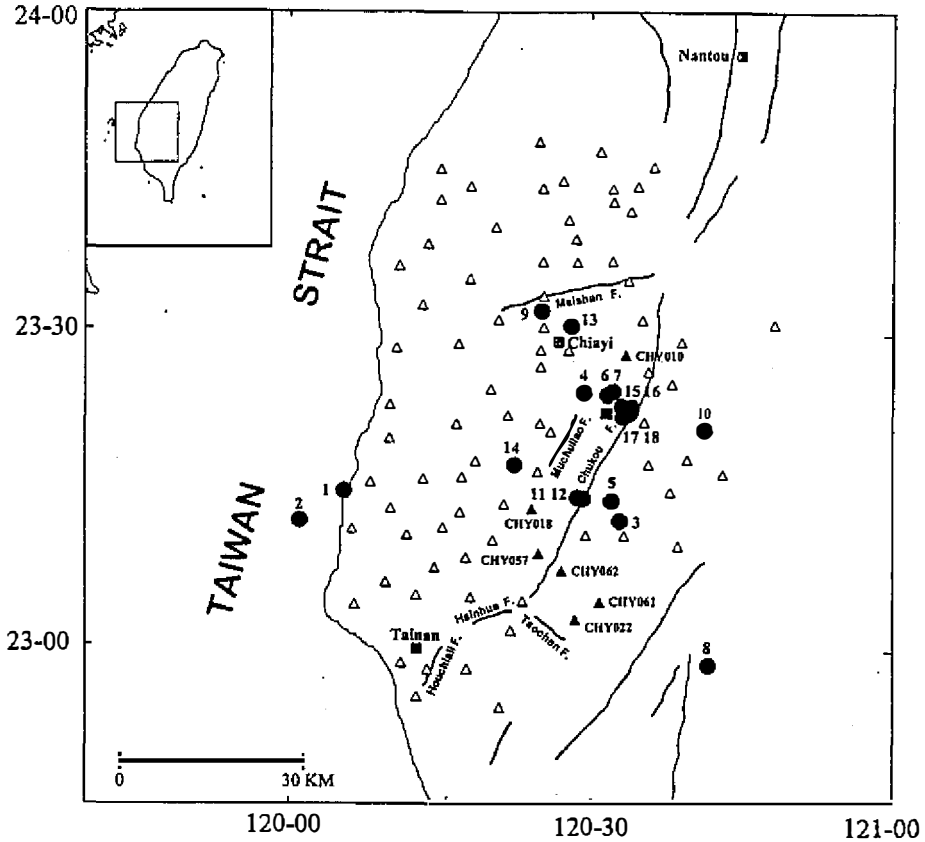
Fig. 1. Location of the strong-motion stations and the mapped fault traces in the CN area. Solid square denotes the rock-site station of CHY087. The epicenters of selected events used in this study are plotted as numbered solid circles. The stations (solid triangular) associated with its name (for example, CHY018, and so on) that recorded the ground motions for earthquake of number 5 were also chosen in the determination of the source spectra. Their results are shown in Appendix.

station in the network consists of a triaxial force-balanced accelerometer which is capable of recording with full scale of ±2g. Two types of accelerographs were used: Teledyne Geotech A900 and Terra Technology IDS3600. Both types have a flat instrument response with a high-cut filter at 50 Hz. Their outputs are digitized at each station with 16-bit resolution at 200 and 250 samples/sec, respectively.

The data presented in this paper are from seismic events recorded by station CHY087 which had a Teledyne Geotech A900 digital accelerograph. There are two reasons for selecting this station. The first is that it is installed at a rock site (Yeh et al., 1992), and hence not

only could the site effects be minimized, but also the seismograms are able to contain high-frequency signals. The second is that this station was triggered by various small- to moderate-sized earthquakes. The earthquakes include the seismic events occurring when station CHY087 was part of the NCCU seismic network in 1991 and 1992. During that time, this station was called USH, but was renamed CHY087 in 1993. The location of this station is indicated by a solid square in Figure 1.

To obtain high-frequency motion data, near-source observations from earthquakes are required. For a site near the source, we expected the waves to suffer less from complication over their paths from the heterogeneous velocity structure under the site as well as guaranteeing the enrichment of high-frequency motion to the data used. As distance from the earthquake increases, the attenuation of high-frequency energy makes it difficult to identify events in detail. To this end, a total number of eighteen earthquakes recorded by station CHY087 from 1991 to 1996 were selected for their small hypocentral distances (all within 67 km, 15 within 30 km) and shallow focal depths (<15 km). All events range in magnitude from M_L 2.8 to 5.8 and are distributed within an area bound by 23°-23.6°N and 120°-120.75°E. This area covers the main geological features in the CN area — the Chukou fault system and the Meishan fault system. The numbered solid circles in Figure 1 represent the epicenters of the earthquakes. Information about the events is listed in Table 1. The configuration of the station relative to the various events covers a wide range of azimuthal directions. As can be seen in Table 1, there are two major events. One of them is the Chiali earthquake (12 March 1991, $M_L = 5.7$), which is a strike-slip fault (Shin et al., 1994). The other is the Tapu earthquake (15 December 1993, $M_L = 5.8$), which has a thrust fault mechanism (Shin, 1995; Huang et al., 1996; Huang and Yeh, 1998). The two events, which are of comparable magnitude, are the most significant to occur in the study area in the last 30 years.

Shown in Figure 2 is an example of the representative velocity records along the east-west direction at station CHY087. They are produced through integration of accelerograms for three events: 5, 9 and 11 (see Table 1). Bars indicated the parts of S-waves used for the spectral analysis. In Figure 2, it is found that the S-wave form is considerably more complicated for event 5 ($M_L = 5.8$) than that for event 9 ($M_L = 5.0$) in different source azimuths. We can also find that the complexity of S-wave form occurs only for event 5, but not for event 11 ($M_L = 4.3$). The locations of these two earthquakes are almost the same (see Figure 1). At such a short source-spacing, the effects of anelastic attenuation along the ray path could be identical for the two earthquakes. Hence, the complex nature of S-wave form for event 5 is mainly due to source effect.

3. METHOD

The computational method of the Fourier amplitude spectrum of ground motion $U_{obs}(f)$ for S waves at frequency f from an earthquake is described with reference to the Atkinson and Boore (1995) model, using the following general form:

$$U_{obs}(f) = \Omega_s(f) exp[-\pi fR/Q\beta]P(f), \tag{1}$$

Table 1. Locations of the selected CN events used in this study. D is the focal depth and H is the hypocentral distance. The source parameters of f_0, M_0 and r represent corner frequency, seismic moment and source radius corresponding respectively to each event.

Event no.	Date	Epicenter		D	M_L	H	f_0	$M_0 \times 10^{24}$	r
	yr m d hr min	Lat. (N)	Long. (E)	(km)		(km)	(Hz)	(dyne-cm)	(m)
1	1991 03 12 06 04	23-14.74	120-04.47	12.0	5.7	49.8	0.72 (3.26)*	0.75	1764
2	1991 03 17 04 37	23 10.72	120-00.66	9.7	5.2	66.5	1.92	0.13	658
3	1991 06 23 18 03	23-10.49	120-32.52	10.6	4.6	25.5	4.52	0.01	280
4	1991 08 08 20 22	23-24.95	120-28.18	7.9	3.8	11.8	3.38	0.006	375
5	1993 12 15 21 49	23-12.80	120-31.42	12.5	5.8	22.6	0.63 (3.26)*	1.1	2004
6	1994 01 03 09 03	23-24.58	120-32.11	3.5	4.4	4.7	3.81	0.01	332
7	1994 01 03 09 12	23-24.48	120-32.26	3.8	4.4	5.0	4.26	0.012	298
8	1994 03 28 08 11	22-59.12	120-41.21	14.4	5.4	49.4	1.04	0.25	1223
9	1994 04 06 01 12	23-31.95	120-25.27	13.4	5.0	23.5	2.21	0.15	573
10	1995 01 19 11 39	23-18.53	120-45.65	14.3	4.5	29.7	2.64	0.05	479
11	1995 04 23 02 57	23-14.83	120-27.95	6.7	4.3	17.2	3.79	0.017	334
12	1995 04 23 03 01	23-14.76	120-26.75	6.6	4.3	17.6	3.79	0.017	334
13	1995 09 28 17 57	23-30.45	120-26.75	9.3	4.5	18.2	2.58	0.027	491
14	1995 10 31 22 27	23-17.45	120-21.53	10.7	5.2	22.3	2.06	0.08	616
15	1996 05 23 16 22	23-23.49	120 31.62	2.7	2.9	2.9	4.52	0.0015	280
16	1996 05 24 08 09	23-23.22	120-32.07	3.6	3.0	3.9	4.52	0.0015	280
17	1996 06 01 10 19	23-23.16	120-32.33	6.5	2.8	6.7	4.11	0.002	308
18	1996 06 01 10 22	23-23.21	120-32.38	1.9	3.0	2.7	4.87	0.012	260

* Number in the parenthese indicate the value of second corner frequency.

where $\Omega_s(f)$ is the earthquake source spectrum for a specified seismic moment, R is the source to station distance, Q is a dimensionless average quality factor for S waves that describes the anelastic attenuation, and $P(f)$ is the high-cut filter that accounts for the observed spectral amplitudes rapidly decay at high frequencies. The high-cut filtering process is important because it controls the ground motion at high frequencies, even at very short distances for a hard-rock site (Hanks, 1982; Anderson and Hough, 1984).

The input parameter of the earthquake source spectrum $\Omega_s(f)$ for the method was modified slightly from that of Atkinson and Boore (1995). Seismic wave theory predicts that the spectral amplitude of source S-wave spectra, for displacement, plateaus at low frequencies and decays in inverse proportion to some power of frequency beyond the corner frequency (e.g., Aki, 1967; Brune, 1970; Sato and Hirasawa, 1973; Molnar et al., 1973). The source

EW Comp.
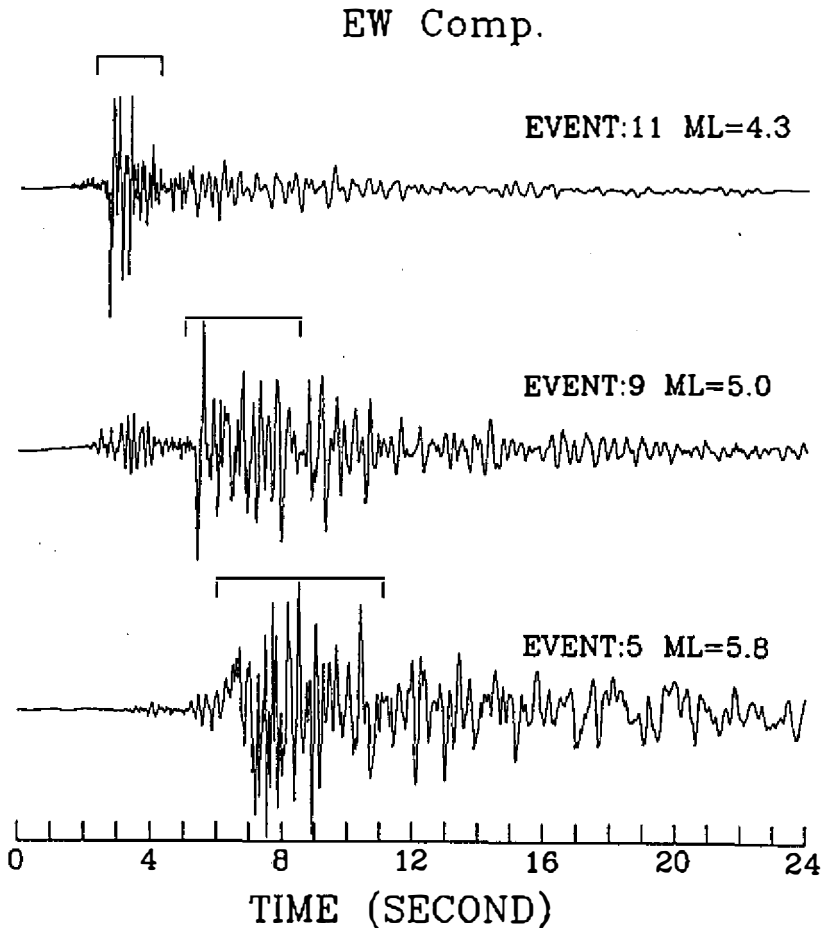
Fig. 2. Examples of velocity seismograms of east-west component integrated from accelerograms at station CHY087 for events of number 5 ($M_L =$ 5.8), 9 ($M_L = 5.0$) and 11 ($M_L = 4.3$), respectively. Vertical scale is unimportant for the purpose of this figure. Bars indicate that the parts of S-waves used in the spectral analysis.

spectra of S waves for a given seismic moment, M_0, which characterizes the above spectral features can be expressed as follows:

$$\Omega_s(f) = \frac{0.781}{4\pi\rho\beta^3 R} \frac{M_0}{[1+(f/f_0)^p]^{-q}}. \qquad (2)$$

In equation (2), f_0 is the source corner frequency, ρ and β are density and shear wave velocity of the source volume. The constant of 0.781 accounts for the average value of shear

excitation 0.55 (Atkinson, 1993; Atkinson and Boore, 1995), together with the free-surface effects of 2.0 and the partition of a vector into horizontal components $1/\sqrt{2}$. For events in the CN area, we used values of $\rho = 2.6\,\text{gm/cm}^3$ and $\beta = 3.4$ km/sec for the density and shear wave velocity, based on the average focal depth (≈ 8 km) for the earthquakes and the crustal model by Yeh and Tsai (1981). From equation (2), the high-frequency decay rate is related to the dynamic properties of the seismic source, which is given by $\gamma = pq$. Here, p and q are positive constants. The ratio of p to q relates the behavior of the spectrum at the intercept of the high and low frequency near to the corner. For a small ratio of p/q, gradual decay begins at frequency somewhat lower than that of the corner frequency and the rate increases until the final value is attained at higher frequency.

In mapping the observed spectrum back to the source spectrum, equation (1) incorporates all the effects anticipated for $U_{obs}(f)$. However, there is a question concerning this method, and that is site effect. Humphrey and Anderson (1994) and Anderson et al. (1996) pointed out that site effects can cause variability in the spectrum due to seismic structure near the recording site, even though the station is located on rock. The work of Ou and Tsai (1995) quantified an average site response at several CN stations by a linear inversion method. Their results indicated that the site response at station CHY087 is relatively flat from 0.4 to 30 Hz; this implies that near-site effects due to impedance contrasts are negligible in the present study.

Proceeding to estimate the source spectra, we first calculate the S-wave displacement-amplitude spectra for two horizontal components for each event. A data sequence was windowed from the onset of the S phase to a point at which 95% of the shear wave energy was contained in the window. The spectra estimated from the truncated time series are determined using a Fast Fourier Transform (FFT). To reduce leakage in FFT estimation, a rectangular cosine taper was used over 10% of each end of the data. Each S-wave spectrum on the log (amplitude) versus log (frequency) display in this paper is calculated from the square root of the sum of two horizontal components. Our next step is to examine the influence of currently used Q models in the region to remove its effects from the spectra. In the third step, a proper choice of p and q was investigated to describe the high-frequency decay rate of the spectrum. Finally, trial values of the seismic moment and stress drop are selected for each earthquake by fitting a model spectrum of equation (2) with the envelopes for the observed spectra.

4. ANALYSIS AND RESULTS

4.1 The Observed Spectra

Figure 3 depicts an example of observed displacement-amplitude spectra of S-waves for seven events of $M_L = 3.0$ to 5.8 with increments of approximately 0.4 magnitude units (exception of $M_L = 3.4$). The effect due to geometrical spreading has been considered by multiplying the spectral amplitude by hypocentral distance R. A remarkable feature in Figure 3 is the similar decay rate of spectral amplitudes for events independent of the epicentral distance and azimuth, although there is some variation in their details. Generally, the spectral amplitudes decrease as f^{-2} at high frequencies (≤ 10 Hz). It is also found that the spectrum without
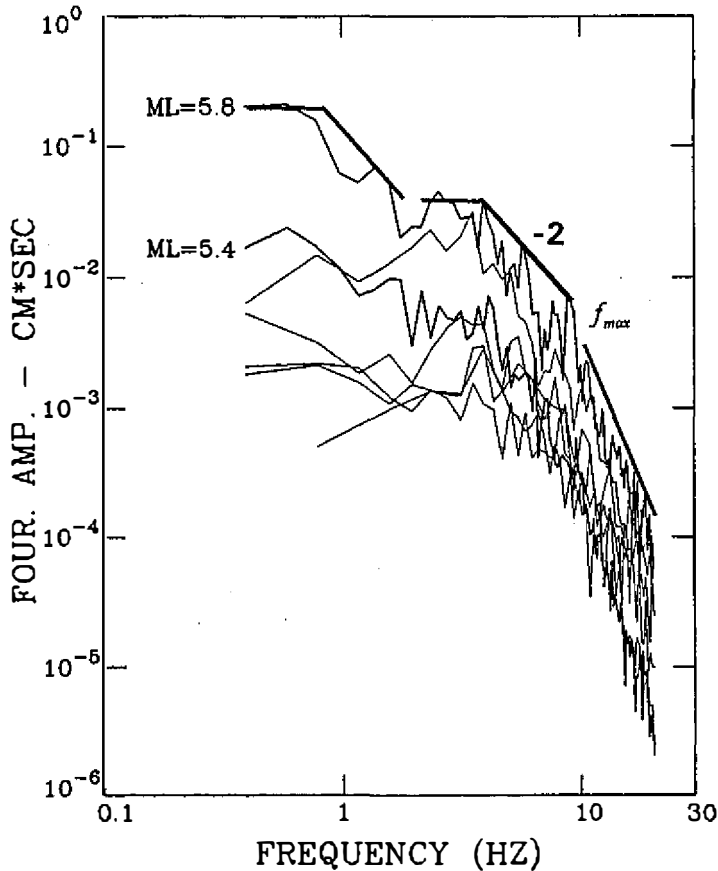
Fig. 3. Observed S-wave displacement-amplitude spectra from local earthquakes with $3.0 \leq M_L \leq 5.8$ that differ in size by approximately 0.4 magnitude unit near station CHY087. The spectral shapes are similar despite the variations of the low-frequency level and the corner frequency.

attenuation correction for earthquakes of $M_L < 5.4$ (thin line) has one corner frequency. However, this feature seems to begin to change as magnitude nears 5.4. As magnitude increases to 5.8, the spectral shape has two corner frequencies (heavy lines), where the spectral envelope changes its general trend.

Another feature shown in Figure 3 is that for frequencies greater than a certain frequency (denoted as f_{max}), spectral amplitudes decay more rapidly than f^{-2} as frequency increases. This decay is often modeled by a high-cut filter of $P(f)$ as in equation (1). Descriptions of $P(f)$ may be suggested by either the f_{max} model (Hanks, 1982) or the kappa (denoted κ) model (Anderson and Hough, 1984). Both the f_{max} and κ representations act to filter out high-frequency motions; their behaviors can be proposed as corresponding respectively to

$P(f) = \left[1 + (f/f_{max})^8\right]^{-0.5}$ (Boore, 1986) and $P(f) = e^{-\pi \kappa f}$ (Anderson and Hough, 1984). The physical origin of f_{max} or κ is still unsolved. There is some debate among many authors as to whether f_{max} is due to source properties (e.g., Papageorgiou and Aki, 1983; Singh et al., 1987; Aki, 1987; Papageorgiou, 1988) or the effects of local site conditions (e.g., Hanks, 1982; Anderson and Hough, 1984). Atkinson (1996) noted that κ might possibly have both source and site effects. It has previously been mentioned that station CHY087 has a relatively flat site response up to frequency of 30 Hz (Ou and Tsai, 1995). This suggests that the apparent high-frequency decay of displacement spectra (Figure 3) for several CN events may possibly arise from the source effect. More evidence is needed to understand the factors that influence the observed high-frequency spectral shapes. Examining the origin of f_{max} (or κ) using seismographic data is not the main purpose of this article. For the present calculation, we therefore chose to use the f_{max} filter from Boore (1986) for the high-cut filter process. For the displacement-amplitude spectra, beyond f_{max} the spectral levels begin to drop even faster; for the acceleration-amplitude spectra, the spectral levels diminish abruptly when $f > f_{max}$. Figure 4 shows a typical observed horizontal acceleration spectrum for the 15 December 1993 Tapu earthquake. In this case, the estimated value of f_{max} is 12 Hz. For the eighteen earthquakes in this study, f_{max} ranged from 8 to 18 Hz.

4.2 The Effect of Attenuation

The source spectrum is usually distorted due to anelastic attenuation, which is in an exponential function as described in equation (1). The anelastic attenuation also influences the high-frequency decay rate of spectral amplitudes. However, the Q value representing anelastic attenuation cannot be determined exactly. Uncertainty in the measurement of the Q value makes it difficult to estimate the corner frequency accurately. This can lead to inaccuracy in estimates of seismic source parameters. Hence, the use of a proper Q value is important. Since our data sets for earthquakes are all for shallow events (<15 km) and are located in a confined region, the effects of anelastic attenuation may be considered identical for all earthquakes.

There have been numerous reports on the determination of the value of Q for the Taiwan region (Shin et al., 1987; Wang, 1988; Wang et al., 1989; Chen, et al., 1989; Wang and Liu, 1990). An important review of the subject was made by Wang in 1993. Together with the results from the above studies, Wang (1993) revised the Q values currently in use into six provinces based on geological and geophysical considerations. One of the provinces is western Taiwan including the Western Foothill and the Coastal Plain. According to the part of seismograms used for the present study, three values of Q were chosen from Table 1 in Wang (1993):

$$Q_c = 260 \sim 300, \text{ for all frequencies (Shin et al., 1987)} \tag{3a}$$

and

$$Q_\beta = 110, \text{ for 2Hz} < f < 6\text{Hz (Wang, 1988)} \tag{3b}$$

for western Taiwan, and
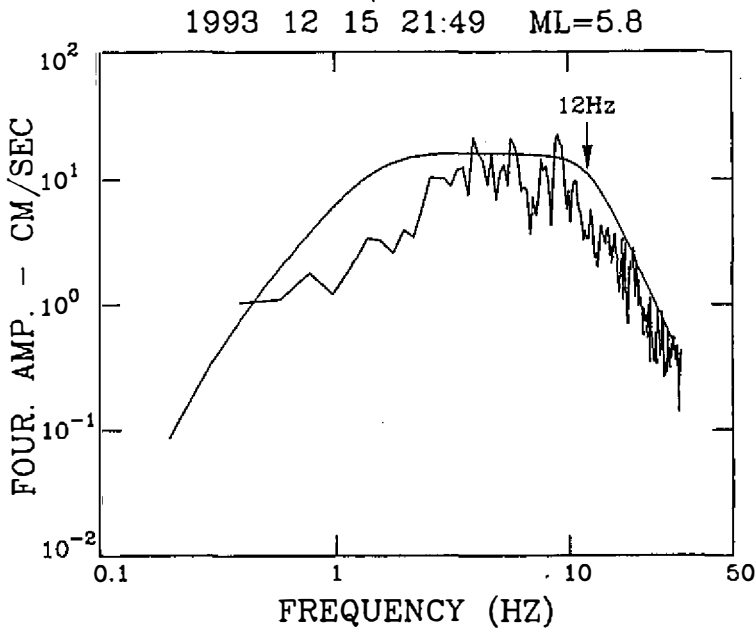
Fig. 4. Example of the observed Fouier acceleration spectra of S-wave for the December 12, 1993, Tapu earthquake recorded at station CHY087. f_{max} is estimated as indicated by an arrow at 12 Hz.

$$Q_c(f) = 117 f^{0.77} \text{ , for } 1\text{Hz} < f < 10\text{Hz (Chen, et al., 1989)}$$ (3c)

for the whole Taiwan region. Although Q_c in equation (3c) may be considered as an average value over a wide region, it can be evaluated in the local region (CN). Here Q_c is the Q value for coda waves and Q_β is the Q value for shear waves.

Typical source spectra for two earthquakes, event 5 ($M_L = 5.8$) and event 6 ($M_L = 4.4$), are shown in Figures 5(a) and 5(b), respectively. The focal depth is 12.5 km for the first event and 3.5 km for the second. The spectra in Figure 5 are corrected for the effect of anelastic attenuation using the three Q values mentioned above. The straight line with a slope of -2 attending the high-frequency envelope for spectra corrected by Q_c from Chen et al. (1989) is used as a reference to compare with the results evaluated from the other two Q values. From these spectra, we can see the shape of the spectra is not very sensitive to Q_c. However, the spectra in Figure 5(a) are particularly large when Q_β is taken into account at frequencies higher than 7 Hz. This is because the high-frequency level of the spectrum is resulted from the band-limited (2 to 6 Hz) avaialable for the Q value in Wang's (1988) results. Comparison of these curves indicates that the frequency-dependent function of the Q value described by Chen et al. (1989) is preferred. This is due to the f^{-2} slope for the high-frequency end of the curve shown. Further evidence is that this Q function is suitable for explaining the source spectra for
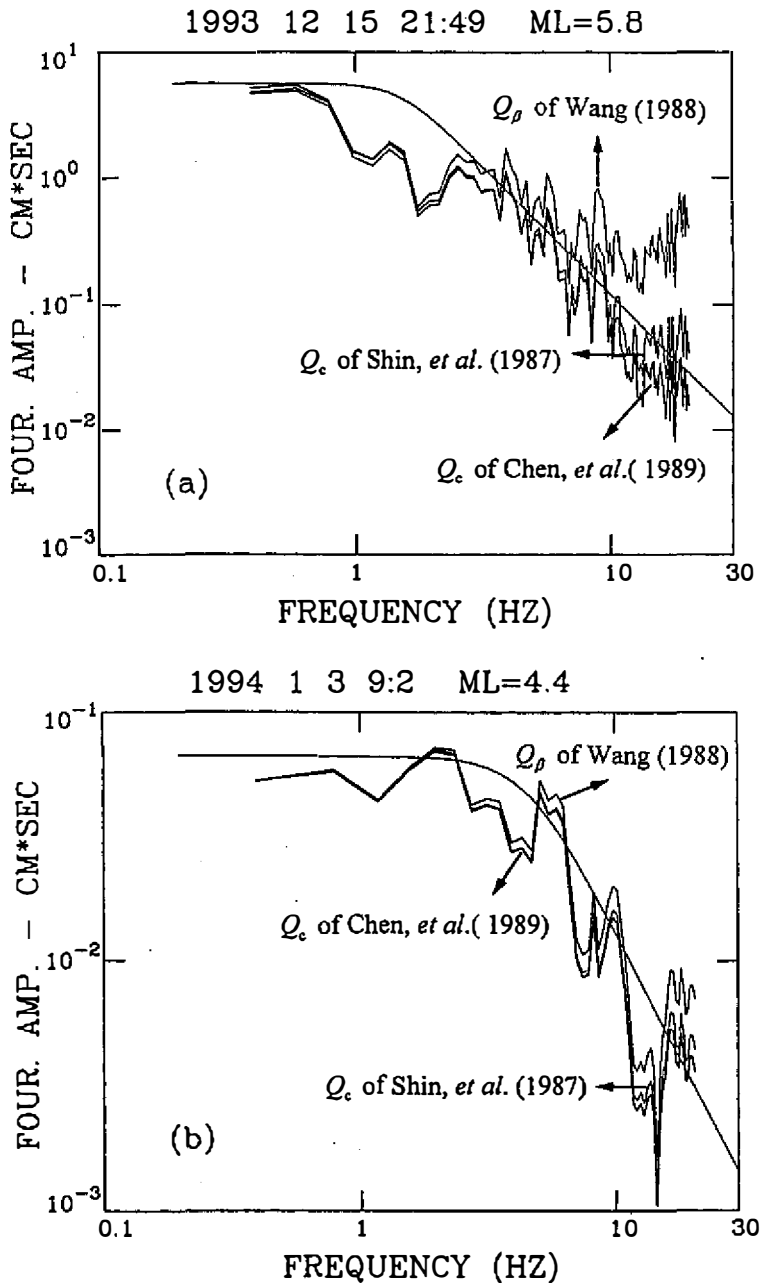
Fig. 5. Examples showing the source spectrum for various choices of Q models for events of (a) the 15 December 1993 (M_L = 5.8), and (b) the 1 March 1994 (M_L = 4.4). The curve shows spectrum corrected for geometric spreading and for anelastic attenuation with $Q_c = 117 f^{0.77}$(Chen et al., 1989), Q_β=110 (Wang, 1988) and Q_c=300 (Shin et al., 1987).

both shallow (≈ 3.5 km) and deep events (≈ 12.5 km) in this case, even though such a function is an average over the whole Taiwan region.

As shown in Figure 5(a), two corner frequencies are still found on the source spectrum for the event of $M_L = 5.8$, while the event of $M_L = 4.4$ only has one corner frequency, suggesting that the attenuation correction does not strongly affect the spectral behaviors, as displayed in Figure 3. This result is consistent with the notion that the existence of two corner frequencies on the displacement-amplitude spectra for the earthquake $M_L = 5.8$ is due to the complex faulting process rather than path effect.

4.3 Spectral Characteristics and Source Parameters

Having a better understanding of attenuation, we can correct the observed spectrum back to the source. Figure 6 displays the source spectra for each event, and these have been corrected for overall attenuation as the product of the geometric and whole-path anelastic attenuation of Q_c (Chen et al., 1989). In Figure 6, all events of $M_L < 5.4$ have spectra with two asymptotic lines (one horizontal and the other inclined with a slope of -2) that intersect at a corner frequency f_0 (i.e., the shape of the Brune model). However, these properties for spectral shape are disrupted for events of M_L approaching 5.4. As the magnitude increases to 5.4, the spectra depart from the shape of Brune model. This feature will be dominant as the magnitude approaches 5.8 (events 1 and 5). Notice that the shape of these spectra is generally characterized by three basic trends which intersect at two corner frequencies f_0 and $\hat{f}_0$, where $\hat{f}_0$ denotes the higher one. At low frequencies the spectrum remains at a relatively constant level. Between the corner frequencies and the spectra decay as an intermediate trend, and beyond $\hat{f}_0$ the slope of the inclined asymptote behaves as f^{-2}.

On the basis of theoretical work on source models, several studies (e.g., Haskell, 1964; Brune, 1970, 1971; Savage, 1972; Sato and Hiwasara, 1973) have used the (lower) corner frequency f_0 to determine the source size. Because all the events in this study are shallow earthquakes, we assumed these earthquakes have ruptured from circular faults. Based on this assumption, the most simple and widely adopted model for general quantification of earthquake sources is the ω-squared model of Brune (1970, 1971). Brune (1970) proposed a circular crack model with an instantaneous stress pulse to produce a displacement spectrum with a f^{-2} falloff. The high-frequency level of the source spectrum is controlled by stress drop, whereas the low-frequency is proportional to the seismic moment. From Burne (1970) model and later later revised (Brune, 1971), the f_0 for shear wave spectra is related to the source radius r as:

$$f_0 = 0.37 \, \beta / r \ . \tag{4}$$

Another parameter which describes the spectrum of earthquake source is the stress drop, $\Delta\sigma$. Brune related this stress drop to the static (global) stress drop from the standard circular static crack solution by Keilis-Borok (1959) and it can be expressed in terms of the well-known relation between seismic moment and corner frequency by:
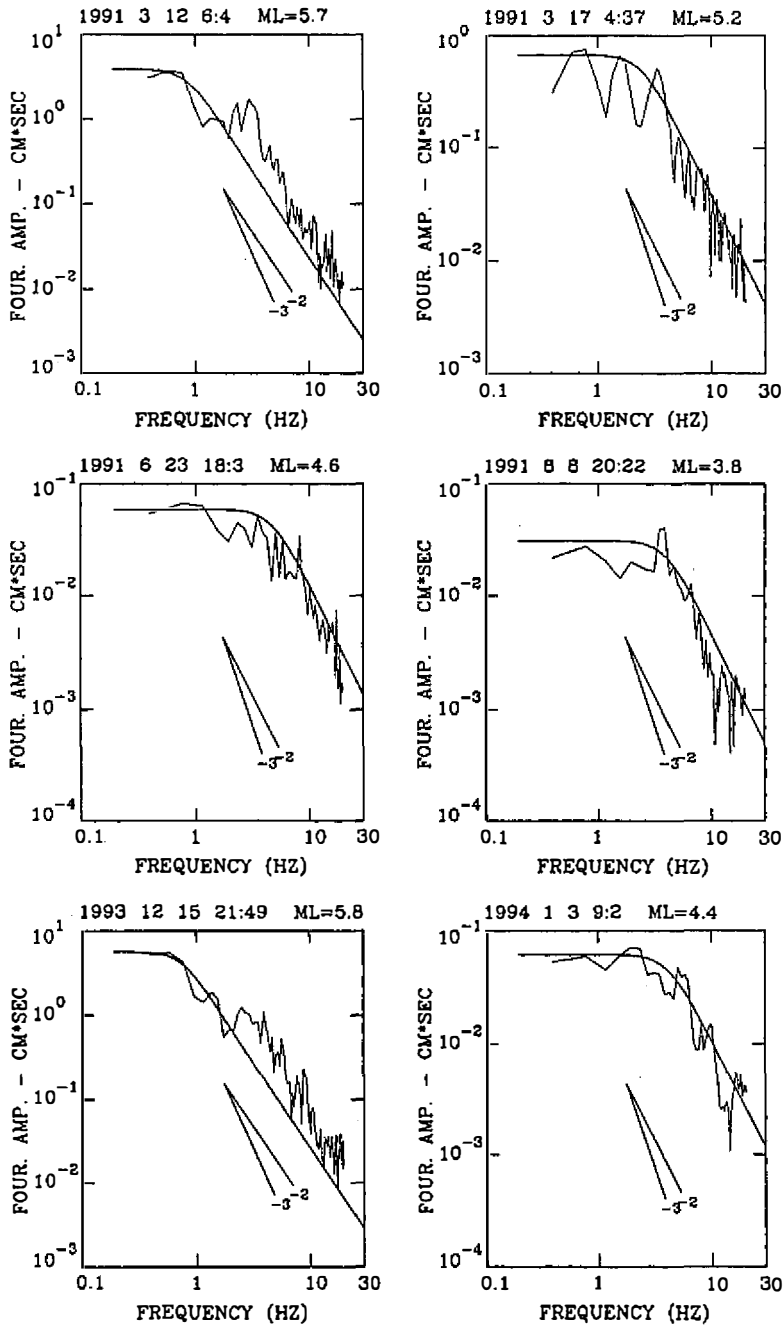
Fig. 6. The source spectrum for the 18 events used in this study. The smooth curve represents the theoretical model of Eq. (2) and was fit to the envelpoe of the spectrum for an assumed seismic moment with a constant stress drop.
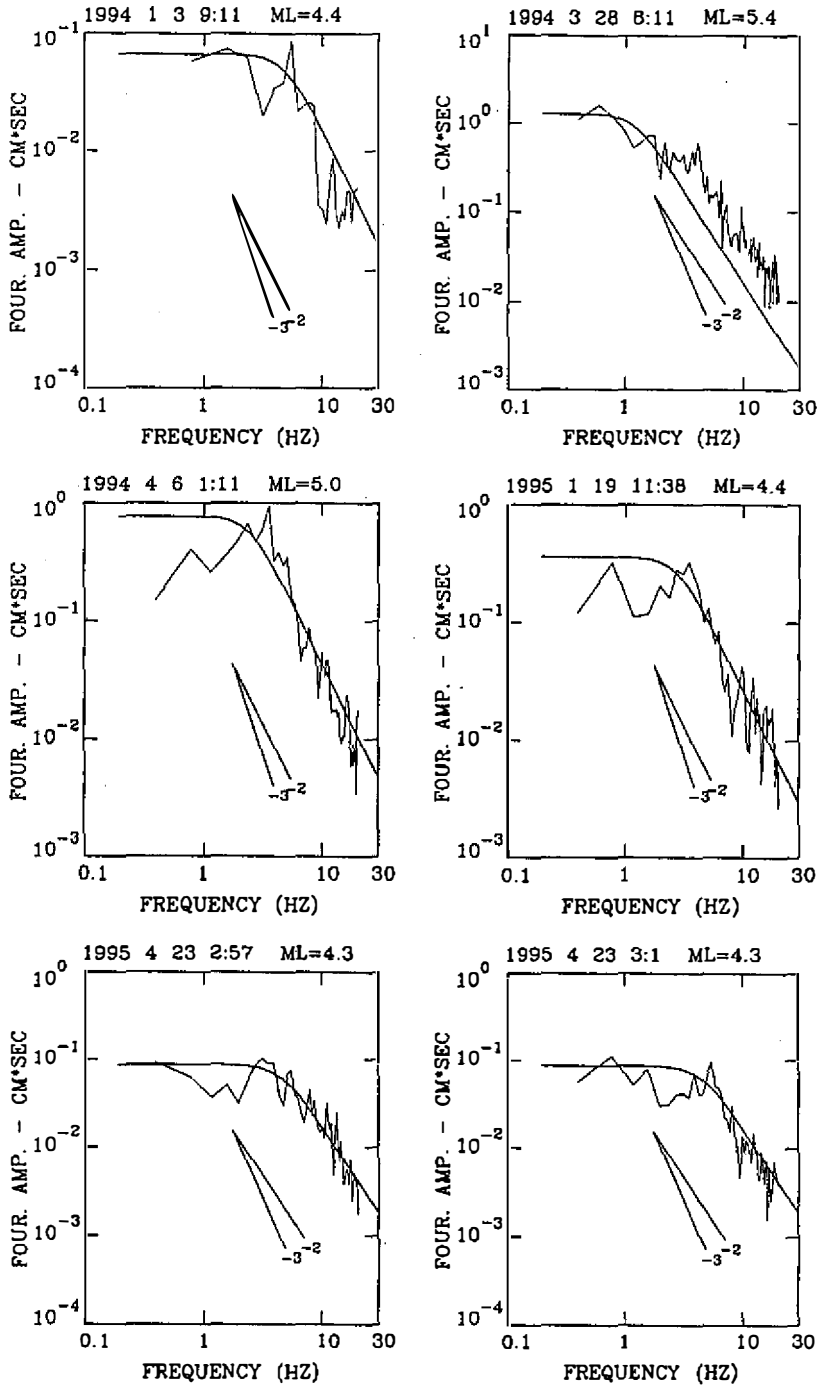
(*Fig. 6.* continued)
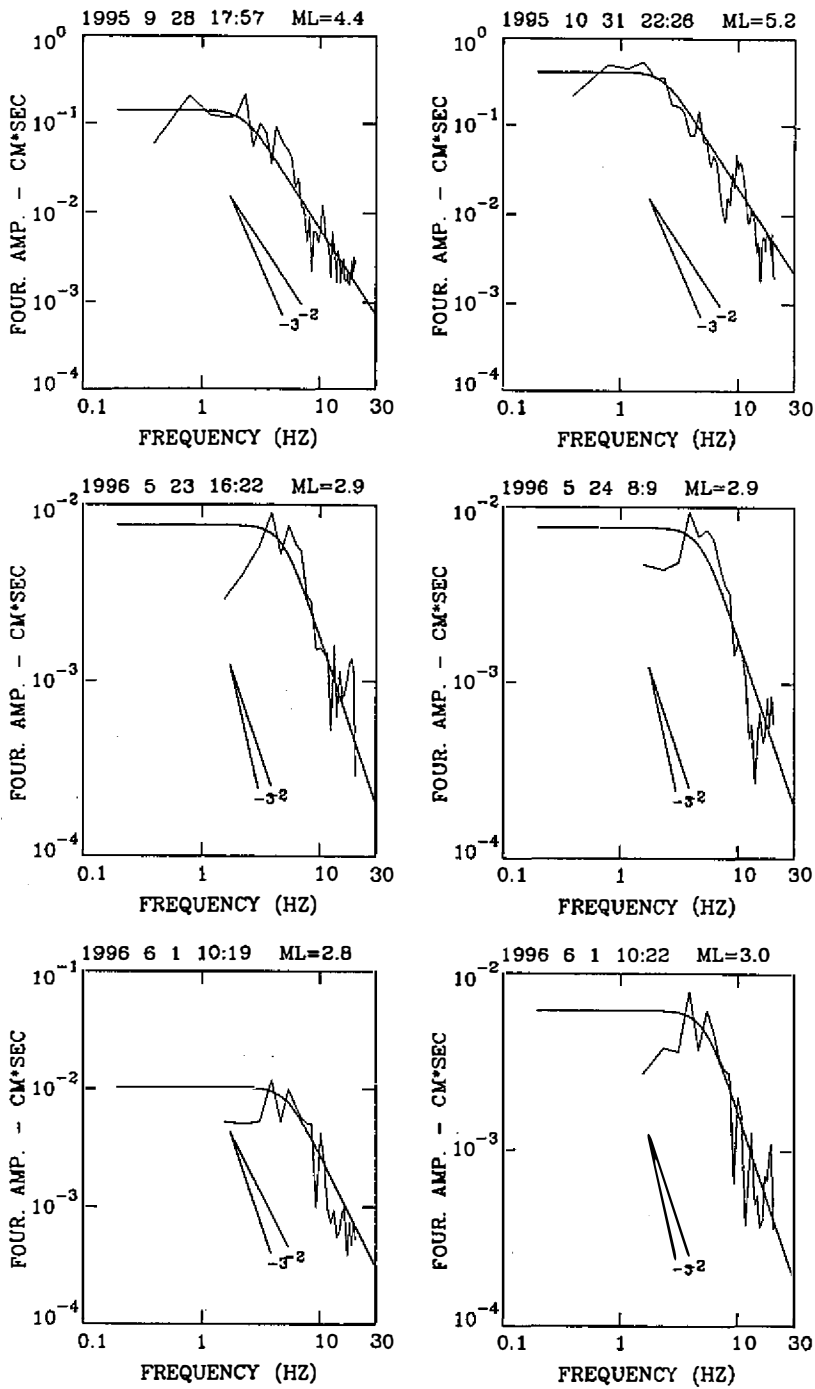
(*Fig. 6.* continued)

$$\Delta\sigma = 8.5 M_0 \left(f_0 / \beta\right)^3. \tag{5}$$

For a constant stress drop, $\log M_0$ is proportional to $\log f_0$ with slope -3. As stress drop increases for an earthquake of a given moment, so does f_0, and the high-frequency level of the source spectrum (see Eq. 2).

So far, the only parameters that take values appropriate to each earthquake source spectrum are seismic moment and stress drop. To estimate both parameters, the theoretical function form of Eqs. (2) and (5) were fit to the source spectra of S waves for an assumed seismic moment with a constant stress drop. At present, there is some ambiguity regarding the identification of the location of f_0. This uncertainty is because stress drop is proportional to the cube of corner frequency. We know that the parameters of p and q in equation (2) are related to the behavior of the spectral shape at intermediate frequencies near the corner frequency and their product is related to the high-frequency decay rate of the spectrum. To clearly demonstrate the corner frequency, tests were carried out for various sets of p and q until the theoretical spectra were best fit to the observed spectra. In the tests, the choice of values of p and q was somewhat arbitrary; however, they can be interpreted in two ways. One of these is that both parameters were dictated by Sato and Hirasawa (1973), Madariaga (1976) and Masuda et al. (1977). They demonstrated the ranging of p from 4 to 10 and of q from 0.2 to 0.5. The second one is that the S-wave spectrum inclined with slope 2 at high-frequency, as shown in Figure 6, appears reasonably fixed at $pq=2$.

Figure 7 shows an example of the fit of the theoretical spectrum to the source spectrum of event 3. To illustrate this comparison, we consider three sets of values of p and q: (i) $p=2$, $q=1$; (ii) $p=4$, $q=0.5$; and (iii) $p=10$, $q=0.2$. For the first set with $p=2$ and $q=1$, equation (2) represents the idealized Brune displacement spectrum. At this point, it should be noted that the $pq=2$ of each set would produce a source spectrum exhibiting a f^{-2} shape at high-frequency as it as in Figure 6. For these cases, the ratio of p/q increases from 2 to 20. As seen in Figure 7, the difference in spectral shape due to the p/q ratio is apparent only around the corner frequency. Comparing the theoretical spectra with the observed spectra, we found that the constructed shape of the source spectrum using $p=4$ and $q=0.5$ (curve b) seems to fit the data at the locus of f_0 better than the other curves. For a lower p/q ratio of 2 (curve a), the transition from the low frequency plateau to the high frequency plateau is expected to be smoother. Nonetheless, the spectrum for intermediate frequencies is enhanced. As increasing the p/q ratio to 20 (curve c) results in the transition around the corner of the spectrum being sharper, this would produce an increase in amplitudes at intermediate frequencies. As mentioned in section 4.1, the similarity in spectral shape for high-frequency decay rate in Figure 3 implies that dynamic processes are common for this group of earthquakes. The parameters p and q are related to the dynamic properties of the seismic source, and thus may be fixed at common values for all earthquakes. In the succeeding analysis, the theoretical predictions of the spectral shape are representative for a set of values of $p=4$ and $q=0.5$ for each individual earthquake.

Since we have assumed the ω-squared model for the source, the spectral parameter, M_0, can be simultaneously obtained from the source spectral amplitude at low frequency while searching to obtain $\Delta\sigma$ at high frequencies. From the estimated moment and stress drop, we
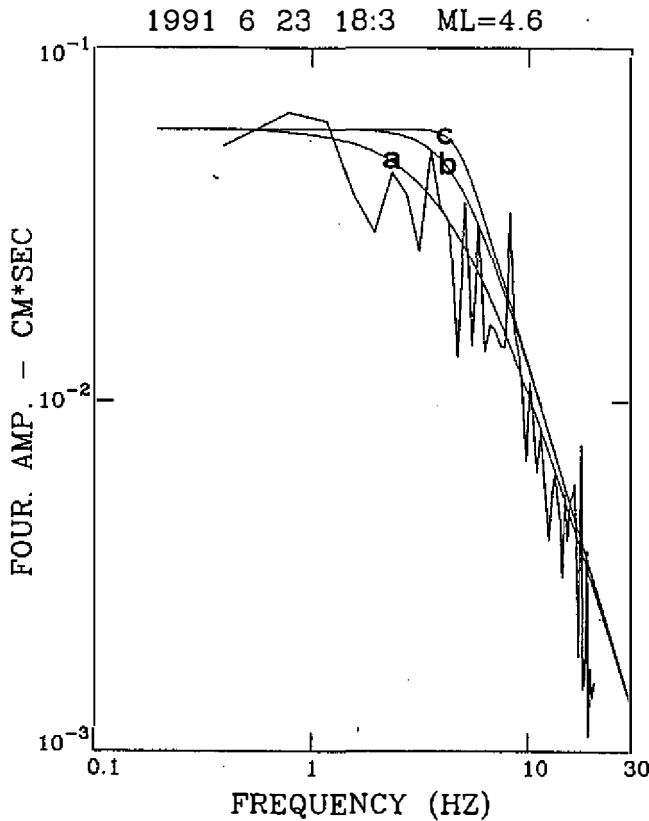
Fig. 7. Comparison of the source displacement spectrum of event 3 with theoretical source spectrum of Eq. (2) for three sets of values of p and q : (a) $p=2$, $q=1$; (b) $p=4$, $q=0.5$; and (c) $p=10$, $q=0.2$. $\gamma = pq$ fixed at 2.

determine the corner frequency for each event. In Figure 6, the smooth line represents the best fit of theoretical spectra to the envelope of observed spectra. The results obtained by the method for this group of earthquakes yield seismic moments in the range of 1.2×10^{21} to 1.1×10^{24} dyne-cm and stress drops from 30 to 350 bars. The corner frequencies f_0 may then be estimated and these vary from 0.63 to 4.87 Hz. Based on equation (4), the source radius of the equivalent circular fault plane is between 260 and 2005 meters. Estimated values of source parameters for the events in this study are summarized in the last three columns in Table 1.

Seismic moment is plotted as a function of corner frequency in log-log scale, and these results are presented in Figure 8 (a). It can be seen that both M_0 and f_0 align with a very small scatter. Using the least-square method, the straight line shows the trends of M_0 and f_0 can be fitted by the following equation:

$$\log_{10} M_0 = -2.95 \log_{10} f_0 + 23.6, \text{ for } 2.8 \le M_L \le 5.8. \tag{6}$$

This linearity can be explained in term of constant stress drop irrespective of seismic moment. On average, the observations agree with this proportionality with slope -3. The relation between seismic moment and radius is shown in Figure 8(b), along with lines of constant stress
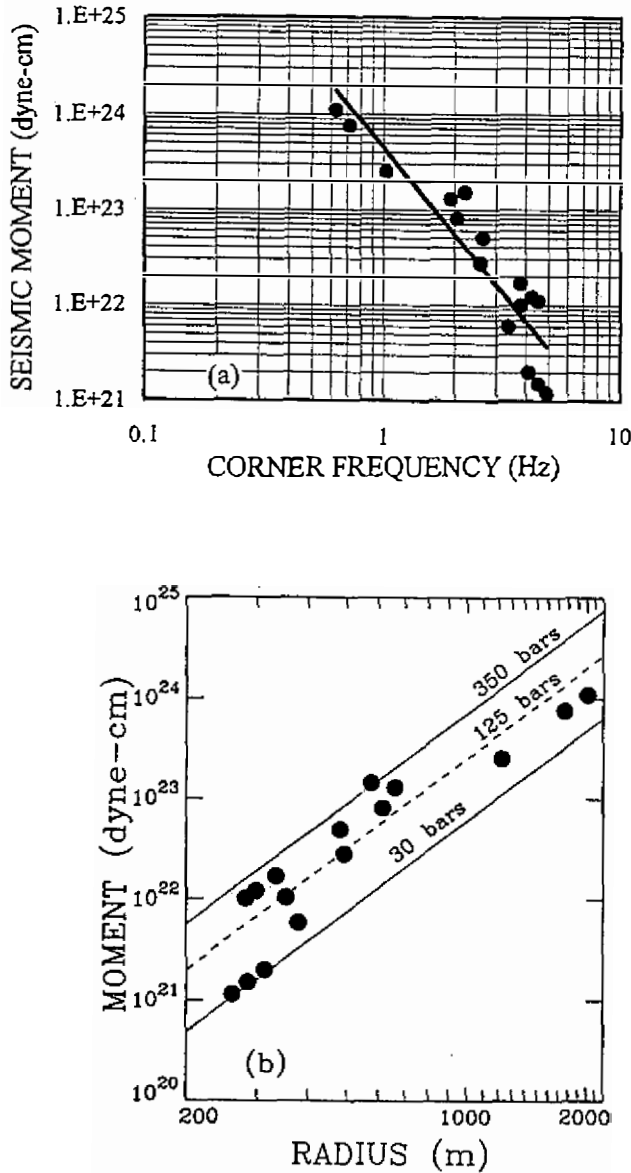
Fig. 8. Relationship between (a) log(seismic moment) versus log(corner frequency), and (b) log(seismic moment) versus log(source radius) for the 18 CN's earthquakes.

drop from 30 to 350 bars. An average stress drop of 125 bars (broken line) is indicated for the earthquakes.

From the function form of Brune (1970, 1971) and a non-linear, least-square simplex algorithm, Ou and Tsai (1993) also obtained the relation of $M_0 - f_0$ in the CN area:

$$\log_{10} M_0 = -3.09 \log_{10} f_0 + 23.86, \text{ for } 3.6 \leq M_L \leq 6.3. \qquad (7)$$

This relation is in agreement with equation (6), and also supports the constant stress drop scaling, including even the data from separate seismic catalogs. They concluded that these earthquakes have an average stress drop of about 150 bars, which is close to our result.

4.4 Spectra with Two Corner Frequencies

Except for the three large events ($M_L \geq 5.4$), as demonstrated in Figure 6, the spectral shapes of the other fifteen relatively small ones ($2.8 \leq M_L \leq 5.0$) are in agreement with the ω-squared model. Two of the larger earthquakes are the most important ones in the recent years. One of them is the 12 March 1991 earthquake near Chiali and the other is the 15 December 1993 earthquake near Tapu. The spectra of these events not only exhibit two well-separated corner frequencies, but also clearly demonstrate that their high-frequency content is much more abundant than that predicted by the ω-squared model. The fitted low-frequency levels (below f_0) corresponding to seismic moment M_0 of these two events are 0.75×10^{24} and 1.1×10^{24} dyne-cm, respectively. Considering the CMT solutions, the seismic moments of both shocks are about the same with M_0 of 1.5×10^{24} dyne-cm. Although seismic moment in this study is evaluated from the record at one station, it is consistent within a factor of two with the CMT value. In addition, the second corner frequency $\hat{f}_0$ of these two events was also measured. The values of $\hat{f}_0$ for both events are almost equal, being about 3.26 Hz.

The existence of more than one corner frequency on source spectra is supported by evidence observed for most other earthquakes (Papageorgiou, 1988; Boore and Akintson, 1992; Boatwright and Choy, 1992; Atkinson, 1993; Takemura et al., 1993; Boatwright, 1994). They are also demonstrated by the theoretical work on source model in the literature (Savage, 1972; Brune, 1970, 1971; Hartzell and Brune, 1979; Papageorgiou and Aki, 1983; Boatwright, 1988). On the basis of the Savage (1972) and Brune (1970) models, both theories provide for a spectrum in which the average trends are in the middle frequencies. In Savage's model, the two corner frequencies exist for a rectangular fault of length L and width W, as $W \ll L$. Conversely, Brune believes that the introduction of an intermediate trend is due to only a fraction of the effective stress released. In actual fault zones, except where geometrical irregularities are distributed, the faults are not simple homogeneous surfaces that permit idealized rupture propagation. The inhomogeneous faulting processes were recognized by an irregular slip motion over a heterogeneous plane, and they also produce more than one corner frequency on the spectra (e.g., Hartzell and Brune, 1979; Papageorgiou and Aki, 1983; Boatwright, 1988). These heterogeneities are significant to earthquake ground motion because they represent locations of concentrated stress (local stress drop) release of the fault, and rupture proceeds as a series of multiple shocks. Despite the various differences between the models, the results of these studies are consistent with the conclusion that the lower corner frequency of the spectrum is related to the rupture duration of the whole fault, whereas the higher corner frequency may reflect the average scale length of the heterogeneities on the fault plane.

Figures 9(a) and 9(b) show the composite spectra of events 1 and 5 reproduced from
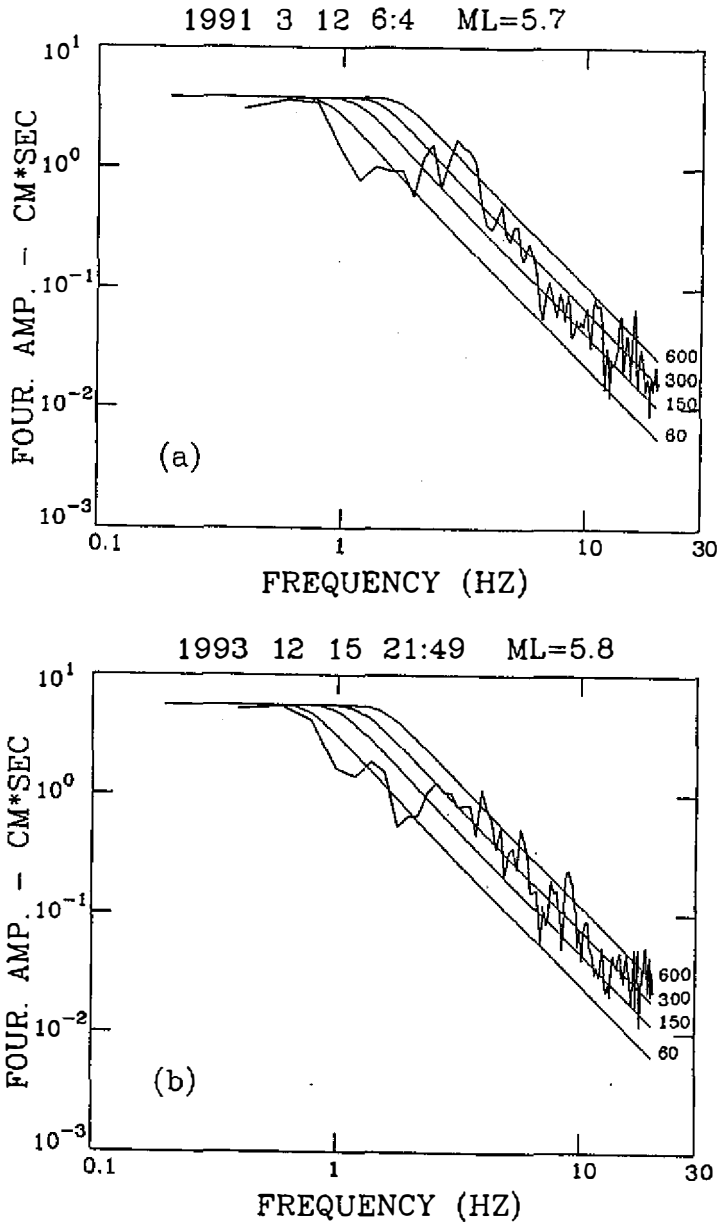
Fig. 9. Source spectrum computed from two mainshocks of (a) the Chiali, and (b) the Tapu earthquakes. The smooth lines represent the idealized spectra for an indicated seismic moment with a different choice stress drop, single-corner-frequency Brune's model. Seismic moment evaluated from the low-frequency spectral level for each event is 0.75×10^{24} and 1.1×10^{24} dyne-cm, respectively. Number at the end of smooth curve denotes the stress drop in bars.

Figure 6. The smooth curves in Figure 9 construct the spectrum for a given moment with stress drops of 60, 150, 300 and 600 bars. It should be noted that two stress drops are required to explain the source spectrum with its general trend. By close inspection of Figure 9, the behavior of the spectrum can be more readily identified. The level at low to intermediate frequencies is matched by a stress drop of 60 bars for both events, and is deficient in amplitude at higher frequencies. In contrast, a high stress drop on the order of 600 bars, much higher than 60 bars, was required to describe the high-frequency level of the spectrum, but the spectral amplitudes in the frequency range 0.63 to 3.26 Hz are considerably higher than the predictions of the ω-squared model.

Analyses of data from the other recordings from the Tapu earthquake were also examined to confirm two corner frequencies on source spectra for this event. Similar trends were identified to data from CHY087 (Appendix).

5. DISCUSSION

We have described local Q values and estimated of source parameters from the observed displacement-amplitude spectra for several CN's earthquakes. To remove the effects of anelastic attenuation as the wave travels along the ray path, the associated Q value of $Q_c = 117\, f^{0.77}$ estimated from the early-arriving coda waves by Chen et al. (1989) was used. The source spectra computation from time windows containing S-wave motion is a crucial question of fundamental relevance to the Q model. As noted by Aki (1981), the attenuation of S waves also has a similar frequency dependence to that of coda waves. Synthesizing these results, Aki (1981) concluded that the coda waves are S-to-S back-scattered waves for locally earthquakes. We adopt this assumption and maintain that Q_c in the CN area is likely to be the Q_β to determine the source spectra. Current uses of the Q function may be considered as an average over the whole Taiwan region. However, this Q function seems suitable to explain the S-wave spectra that are expected to provide some source parameters for the earthquakes in this study. This is likely because not only the f^{-2} slope for high-frequency end of the curve shown in Figure 5, and it is also sufficiently suitable to explain the source spectra for both the deeper (≈ 12.5 km) and shallower (≈ 3.5 km) events.

The relation of $M_0 - f_0$ in both this study and that of Ou and Tsai (1993) supports a cubic relation between source radius and seismic moment, and indicates that the stress drops of crustal earthquakes in the CN area are independent of source dimension compilation of magnitudes in the range of 2.8 to 6.3. Although the values vary for different events, an average stress drop of 125~150 bars appears well-established in this area. It should be noted that the scaling of source spectra in present study was determined by the lower frequency of f_0 and the level of horizontal asymptote. We know that stress drop estimated in this sense is referred to as a global one, which is inferred by assuming the entire rupture area to be uniform over a smooth fault without discontinuities. Although this stress drop estimate provides useful insight regarding the general quantification of earthquakes, locally, however, the stress drop can be much higher than average, and for moderate and larger earthquakes.

This distinction can be seen in Figure 6 because the spectral behavior has a major change

taking place near magnitude 5.4. At magnitudes less than 5.4, the spectra have a readily identifiable corner frequency, followed by a plateau, after which the spectral amplitude has a f^{-2} falloff. This implies that the fault plane is somewhat simpler in character for these small events. It seems clear that for small earthquakes, the fault plane can be considered as a circular crack (a single patch) with smooth-rupture faulting. The obvious evidence for this explanation is that the seismograms with simple S-waves generally can be seen for small events (Figure 2).

On the other hand, for spectra of the two main shocks of the 1991 Chiali and 1993 Tapu earthquakes, the source spectrum departs greatly from the assumed Brune's spectral shape. These two earthquakes are characterized by the high-frequency source spectra shown in Figures 9(a) and 9(b). An interesting observation concerning the spectra is that the data are associated with two-corner-frequency in place of the single one of the Brune's model. It was suggested that for events with two corner frequencies may have come across some obstacles during the faulting. This explanation is supported by the fact that the time domain records of earthquakes show that the S-wave waveforms are relatively complex, at least on the time scale of 1 to 5 sec (Huang and Yeh, 1988). In order to fit the high-frequency spectral amplitudes with the commonly used ω-squared model, we further found that a high stress drop of about 600 bars (or perhaps somewhat greater) deduced from the earthquakes is about 10 times as high as the average stress drop (*ca.*, 60 bars). As pointed out by Wald et al. (1993), variations in tectonic stress can be large over a scale length to a few kilometers, but regions of high and low stress drops are averaged out resulting in stress drops of several tens of bars. This strongly suggests that faulting was initiated with localized but massive faulting with associated stress differences not at all representative of those inferred for the entire faulting process.

Important direct observational evidence, indicating major differences of source spectra between small and moderate earthquakes, has been obtained from the discussion above. The high-stress events accompanied by an anomalous spectral shape may exist for events as large as M_L 5.8. This implies that an ω-squared model with a constant stress drop cannot cover the entire range of seismic spectra in the magnitude range of 2.8 to 5.8. Such a phenomenon would contradict the results obtained by Ou and Tsai (1993), as they indicated that the spectral scaling as a function of magnitude. Consequently, the issue of stress drop for moderate earthquakes has become an acute one for seismic hazards in the CN area. For this reason, the Tapu earthquake on 15 December 1993 is of exceptional interest. This is because the results of previous investigations (Chang and Shin, 1994; Chung and Yeh, 1997; Shin, 1995; Huang et al., 1996; Huang and Yeh, 1998) can be used to examine our analysis.

An attempt to obtain source parameters of the Tapu earthquake utilizing synthetic seismograms to model actual data at near-source distances was first made by Shin (1995) and later by Huang et al. (1996) and Huang and Yeh (1998) using different approaches. The first two studies represented the source as a point. However, in the most recent study, a kinematic complexity in modeling the source time function for a circular fault model with a radius of 2 km was assumed. For this waveform modeling, the seismic moment is determined from the observed amplitude of S waves and its frequency content depends on the pulse width of a source-time function. For a simple circular fault model, the pulse width of the source-time function (τ) is given in terms of the source radius (r) and the S-wave speed (β) by $\tau = 2.62r / \beta$ (Cohn et al., 1982). The stress drop is then estimated to be proportional to the

moment divided by the cube of the source dimension from the circular crack solution as $\Delta\sigma = (7/16)(M_0/r^3)$ (Keilis-Borok, 1959). Following the procedure outlined above, Huang et al. (1996) estimated that the stress drop of the earthquake was about 320 bars based on τ of 1.0 sec, which is about twice as large as the value obtained by Huang and Yeh (1998). With further work, Huang et al., (1996) and Huang and Yeh (1998) found that an exceedingly high stress drop of 2.5 Kbars was predicted using τ of 0.3 sec (Shin, 1995). As discussed by Haung and Yeh (1998), the essential differences among these stress drops may be attributed to the pulse width of the source-time function used. A shorter source-time function produces a decrease in source radius and an increase in stress drop, thus raising questions concerning the validity of the source model for this event.

As a point, we would like to comment on the source area of the Tapu earthquake. Based on the aftershock distribution following this earthquake, Chang and Shin (1994) proposed that this earthquake could have a fault length of 4.0 km and a width of 7.0 km. Following this fault model, Chung and Yeh (1997) assumed a propagation process to simulate the ground motion of short-period surface waves at an epicentral distance greater than 24 km. We disagree with their assumption of a rupture surface because it was determined by the aftershocks occurring with the following 45 days. This definition is somewhat questionable. Most frequently, the aftershock area is defined about one day after the main shock (Mogi, 1967). Thus, the overall distribution of the aftershocks may give an overestimate of the main shock area. In subsequent analysis of the earthquake, Huang and Yeh (1998) demonstrated that the assumption of the rectangular fault model was invalid for appropriately describing the ground motions at shorter distances. Instead of the rectangular fault model, they established that a circular model with 2-km radius could be properly used to explain the observed waveforms and the computed seismograms.

Determinations of the area of the rupture surface (A) have been correlated with seismic moment (M_0) by various researchers (e.g., Kanamori and Anderson, 1975; Prucaru and Berekhemer, 1982). Specifically, the last two authors used a dataset of 240 events ($M \geq 5$) to obtain the relationship $\log_{10}M_0 = 1.5\log_{10}A + 22.5$ for $10^{24} \leq M_0 \leq 10^{30}$, where A is in km^2 and M_0 is in dyne-cm. We assume that A as function of M_0 as expressed in this equation is valid on average. Also, we accept the teleseismic estimate of the moment (1.5×10^{24} dyne - cm) for the Tapu earthquake. Under these considerations, the fault area for the earthquake is about 13 km^2. If we take a circular fault model as the fault plane, the earthquake has a source radius of about 2 km. This can agree perfectly with the source radius obtained by Huang and Yeh (1988), who picked the corner frequency as the intercept of the high and low-frequency asymptotes of the spectra from widely distributed seismic stations. If $f_0 \approx 0.63$ Hz, this yields a source radius of about 2 km for $\beta = 3.4$ km/sec and also supports the validity of a source radius of 2 km. From the above results, the event did not show evidence for such a source as described by Chang and Shin (1994), or by Shin (1995) and Huang et al. (1996). We strongly believe that the source area of the Tapu earthquake is about 13 km^2 with rupture length and width roughly comparable (i.e., a circular crack).

Apart from the source area analysis, a trade-off exists in estimation of stress drop for this event to be significantly too large as shown by Shin (1995) and Huang et al. (1996). Stress drop in the associated derived source spectral amplitude in this article is 60 bars, which is

smaller by a factor of 2 than our 1998 results (Huang and Yeh, 1998). Indeed, neglecting the Q correction in our waveform modeling could cause this overestimate.

Finally, we would like to comment on the subevent size based on observations from the characteristic frequency $\hat{f}_0$ for the Chiali and Tapu earthquakes. The $\hat{f}_0$ is about 3.26 Hz. Using a stochastic fault model, Koyama (1983) deduced that the $\hat{f}_0$ is related to the average scale length ($\bar{d}$) and the rupture velocity (v_r) of the fault heterogeneities as $\hat{f}_0 = v_r / 2\pi\bar{d}$. For an assumed rupture velocity of $v_r = 0.7\,\beta$ (Kanamori, 1994), the estimated average scale length of both events which corresponds to the second corner frequency is about 116 meters.

Papageorgiou and Aki (1983) used a specific barrier model to interpret strong motion data. In this model, they used Sato and Hirasawa's (1973) circular crack model with radius ρ_0 to represent the localized subevents. The ρ_0 is related to the expected values of corner frequency ($\hat{f}_0$) as $\rho_0 = C_s\beta / 2\pi\hat{f}_0$ (where C_s is an implicit function of rupture velocity). Assuming a ratio of $v_r / \beta = 0.7$, C_s is 1.81 (Sato and Hirasawa, 1973), and $\rho_0 = 300$ meters. Interpreting the diameter $2\rho_0$ as the barrier interval, the inferred barrier interval for these events is about 600 meters, which is about a factor of 5 higher than Koyama's model. Considering the four smaller events of M_L around 3.0 in this study (see final entry in Table 1), the averaged value of diameter $2r \approx 564$ meters nearly coincides with the barrier interval of Papageorgiou and Aki's model. If true, this would have important implications for attempts to simulate ground motion from large earthquakes by using small earthquakes as Green's functions (Hartzell, 1978).

For the Tapu earthquake, the scale length enters into the description of the spectra as in the previous section and its associated local stress drop is discussed below. Based on the specific barrier model developed by Papageorgiou and Aki (1983), the local stress drop ($\Delta\sigma$) can be obtained by:

$$\Delta u_{max} / \rho_0 = (24/7\pi)\,(\Delta\sigma/\mu), \tag{8}$$

where Δu_{max} is the maximum relative slip of the faces of an individual crack, which can be represented by $\Delta u_{max} = M_0 / (\pi/6 \times \mu \times A)$ [from equation (57) of their paper] based on their specific barrier model. Here, A is the area of the entire fault plane and μ is the shear modulus. We considered $A = 12.6$ km^2 as described above and assumed $\mu = 3 \times 10^{11}$ dyne/cm^2. Two estimates of Δu_{max} are ≈ 76 cm and 56 cm corresponding respectively to $M_0 = 1.5 \times 10^{24}$ (taken from the CMT solution) and 1.1×10^{24} dyne-cm (this study). Substituting the values into equation (8), we obtain (i) $\Delta\sigma \approx 700$ bars, for $\Delta u_{max} 76$ cm and (ii) $\Delta\sigma \approx 516$ bars, for $\Delta u_{max} \approx 56$ cm. It is noteworthy that the local stress drop of 600 bars, that was constructed based on the level of high frequency obtained for the Tapu earthquakes, falls in this range.

If we considered $\rho_0 \approx 300$ meters as an average scale length on the fault plane for the Tapu earthquake, the total number of cracks which are distributed on the fault plane can be inferred as 12.6km$^2 / (\pi \cdot 0.3$km$^2) \approx 45$ cracks. The total energy E_s radiated by the fault should be equal to the sum of the seismic energies E_{si} radiated from each individual crack. An estimate of E_{si} can be obtained from Sato and Hirasawa's model (1973). Following Sato and Hirasawa's (1973) formula, Papageorgiou and Aki (1983) presented their specific barrier model

with $\alpha/\beta = 1.73$ and $v_r/\beta = 0.75$ to calculate the total seismic energy radiated from the entire fault which is given by:

$$E_s = 0.46 \cdot \frac{1}{2} \cdot M_0 \cdot \frac{\Delta\sigma}{\mu}. \qquad (9)$$

Here, $\Delta\sigma$ represents the local stress drop. From Huang and Yeh's (1998) analysis of this event we know that $\alpha/\beta \approx 1.74$ and $v_r/\beta \approx 0.7$. Both estimates do not vary much from Papageorgiou and Aki's assumption. Assuming that $\mu = 3 \times 10^{11}$ dyne/cm^2 and substituting the estimate of $M_0 = 1.1 \times 10^{24}$ dyne-cm and $\Delta\sigma = 600$ bars from this study in equation (9), we calculate the total seismic energy is $E_s \approx 5 \times 10^{20}$ erg. An estimate of the same quantity also obtained using the Gutenberg-Richter relation ($\log E_s = 1.5M + 11.8$) is $E_s \approx 3.2 \times 10^{20}$ erg.

6. CONCLUSION

We analyzed S-wave source spectra for eighteen events with $2.8 \leq M_L \leq 5.8$ recorded by the CN network from 1991 to 1996. Within a limited range of epicentral distances and a wide range of source-receiver azimuth, the results provide some information on CN earthquakes which is summarized as follows:

(1) The frequency-dependent attenuation of $Q_c = 117f^{0.7}$ proposed by Chen et al. (1989) was found to be in good agreement with those found in the observed spectra for CN earthquakes, whether their depths were deep (≈ 12.5 km) or shallow (≈ 3.5 km) focus.

(2) The source scaling between corner frequency (f_0) and seismic moment (M_0), as shown in Figure 8, is considered to be linear with a slope of -3. This dependence is generally explained in term of a constant stress drop. The overall trend appears to indicate that the stress drops are averaged out resulting in an estimate of 125 bars. Similar results were also obtained by Ou and Tsai (1993). However, the relation in a previous investigation by Ou and Tsai (1993) and in the present work must be justified on the basis of inferences from two moderated-size earthquakes which occurred near Chiali in 1991 (event 1) and near Tapu in 1993 (event 5). The complicated source spectral shape and the enhanced high-frequency of the two main shocks were not reflected in a simple ω-squared model with a stress drop of 125 bars.

(3) The spectral shapes of events 1 and 5 appear to be similar, but distinctly not f^{-2}, which is in clear contrast to the spectra obtained from the $M_L < 5.4$ earthquakes. Apparently two corner frequencies always exist. The intermediate spectral behavior extends from 0.63 to 3.26 Hz. The spectral amplitude below the low frequency of f_0 and this intermediate trend is well described by a stress drop of 60 bars. In contrast, the high-frequency level at the source surprisingly required a stress drop of 600 bars to match it. This observational result implies that the shape of the source as described by the ω-squared model ceases to be valid as magnitude increases up to 5.8 in the CN area.

(4) According to Sato and Hirasawa's (1973) circular rupture model, the scale length (barrier

interval) inferred for the events from higher corner frequency ($\hat{f_0}$) is about 300 meters. This is comparable to the source dimension for small earthquakes of $M_L \approx 3$ selected for this study. The high-frequency decay beyond the second corner frequency associated with a high stress value of 600 bars was verified by the specific barrier model from Pagageorgiou and Aki (1983) and by the energy-magnitude relation from Gutenberg and Richter (1956).

APPENDIX: Source spectra for the Tapu earthquake

S-wave spectra of source at stations of CHY010, CHY018, CHY022 CHY057, CHY061 and CHY062 (solid triangulars in Figure 1) for the Tapu earthquake are corrected for the effect of attenuation due to the ray along the propagation path of seismic waves and for f_{max}. Similar features with a complex spectral shape associated with two corner frequencies, as in Figure 9(b), are apparent from these spectra. This suggests that if we are concerned with the high frequency spectral amplitudes of the earthquakes, source scaling currently in use may underestimate spectral amplitudes for moderate-sized earthquakes in the CN area.

1993 12 15 21:49   ML=5.7

CHY010

1993 12 15 21:49   ML=5.7

CHY061

1993 12 15 21:49   ML=5.7

CHY062

1993 12 15 21:50   ML=5.7

CHY018

1993 12 15 21:49   ML=5.7

CHY022

1993 12 15 21:49   ML=5.7

CHY057
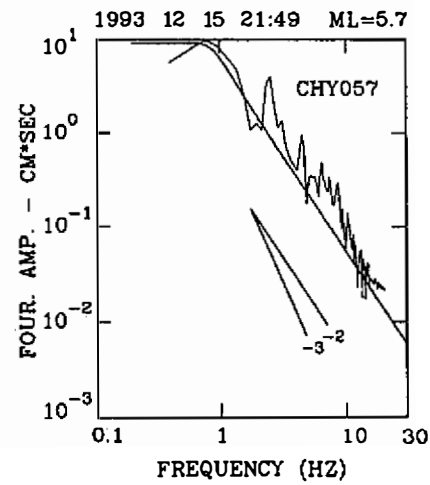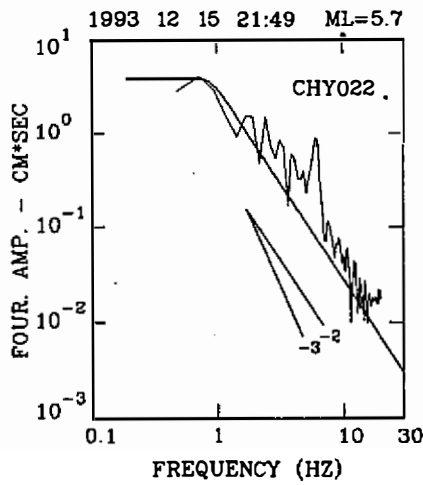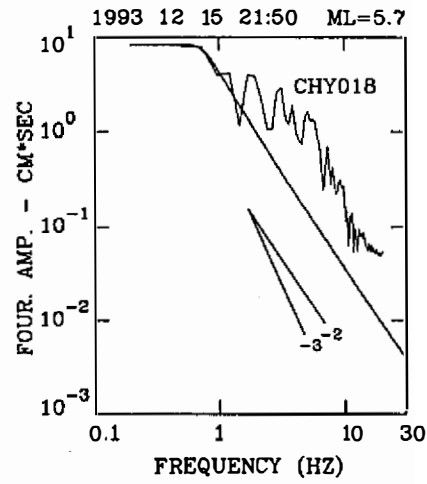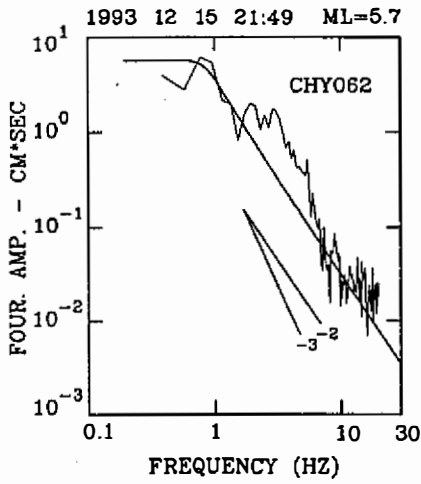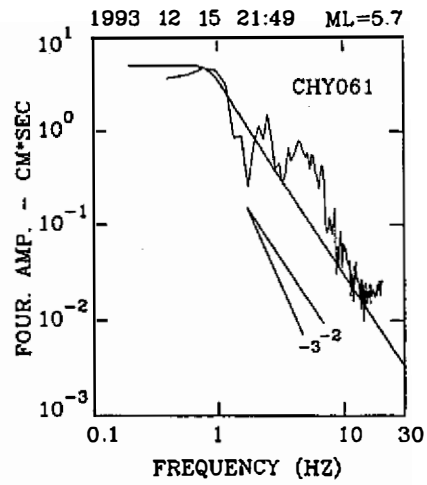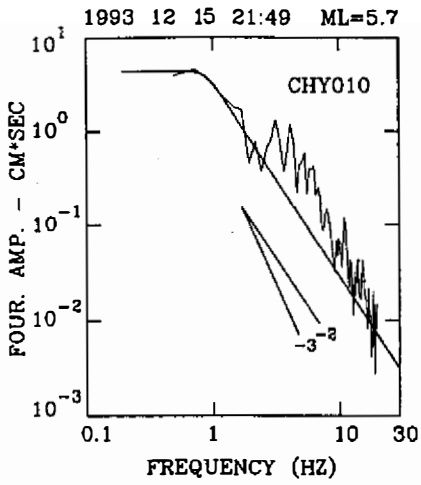
REFERENCES

Aki, K., 1967: Scaling law of seismic spectrum. *J. Geophys. Res.*, **72**, 1217-1231.

Aki, K., 1979: Characterization of barriers on an earthquake fault. *J. Geophys. Res.*, **84**, 6140-6148.

Aki, K., 1980: Attenuation of shear waves in the lithosphere for frequencies from 0.05 to 25 Hz. *Phys. Earth Planet. Interiors*, **21**, 50-60.

Aki, K., 1981: Attenuation and scattering of short-period seismic waves in the lithosphere, in Identification of Seismic Source; Earthquake or Underground Explosion, E. S. Hsuebye and S. Mykkeltveit, Editors, D. Rei, Hingham, Massachusetts, 515-541.

Aki, K., 1987: Magnitude frequency relation for small earthquakes: a clue to the origin of f_{max} of large earthquakes. *J. Geophys. Res.*, **92**, 1349-1355.

Anderson, J. G., and S. E. Hough, 1984: A model for the shape of the Fourier amplitude spectrum of acceleration at high frequencies. *Bull. Seismol. Soc. Am.*, **74**, 1969-1994.

Anderson, J. G., Y. Lee, Y. Zeng, and S. Day, 1996: Control of strong motion by upper 30 meters. *Bull. Seismol. Soc. Am.*, **86**, 1749-1759.

Atkinson, G. M., 1993: Earthquake source spectra in Eastern North America. *Bull. Seismol. Soc. Am.*, **83**, 1778-1798.

Atkinson, G. M., 1996: The high-frequency shape of the source spectrum for earthquakes in the eastern and western Canada. *Bull. Seismol. Soc. Am.*, **86**, 106-112.

Atkinson, G. M., and D. M. Boore, 1990: Recent trends in ground motion and spectral response relations for North America. *Earthquake Spectra*, **6**, 15-36.

Atkinson, G. M., and D. M. Boore, 1995: Ground-motion relations for eastern north America. *Bull. Seismol. Soc. Am.*, **85**, 17-30.

Boatwright, J., 1988: The seismic radiation from composite models of faulting. *Bull. Seismol. Soc. Am.*, **78**, 489-508.

Boatwright, J., 1994: Regional propagation characteristics and source parameters of earthquakes in northeastern North America. *Bull. Seismol. Soc. Am.*, **84**, 1-15.

Boatwright, J., and G. L. Choy, 1992: Acceleration source spectra anticipated for large earthquake in northeastern America. *Bull. Seismol. Soc. Am.*, **82**, 660-682.

Boore, D. M., 1986: The effects of finite bandwidth of seismic scaling relationships. *Proc. of the 6th Ewing Symp.*, American Geophysics Union, Geophysical Monograph. **37**, 275-284.

Boore, D. M., and G. A. Akinson, 1992: Source spectra for the 1988 Saguenay, Quebec earthquakes. *Bull. Seismol. Soc. Am.*, **82**, 683-719.

Brune, J. N., 1970: Tectonic stress and the spectra of seismic shear waves from earthquakes. *J. Geophys. Res.*, **75**, 4997-5009.

Brune, J. N., 1971: Correction. *J. Geophys. Res.*, **76**, 5002.

Chang, C. H., and T. C. Shih, 1994: Earthquakes in 1993. *Meteor. Bull.*, **39**, 202-217.

Chen, K. C., T. C. Shin, and J. H. Wang, 1989: Estimation of coda Q in Taiwan. *Proc. Geol. Soc. China*, **32**, 339-353.

Cheng, S. N., and Y. T. Yeh, 1989: Catalog of the earthquakes in Taiwan from 1604 to 1988. *Institute of Earth Sciences, Academia Sinica*, Taipei, Taiwan, 255pp (in Chinese).

Cheng, S. N., and Y. T. Yeh, 1985: How large for an anticipated earthquake in southwestern Taiwan. *Science Monthly*, Taipei, Taiwan, **18**, 603-608 (in Chinese).

Chung, J. K., and Y. T. Yeh, 1997: Shallow crustal structure from short-period Rayleigh-wave dispersion data in southwestern Taiwan. *Bull. Seismol. Soc. Am.*, 87, 370-382.

Cohn, S. N., T. L. Hong, and D. V. Helmberger, 1982: The Oroville earthquake: A study of source characteristics and site effects. *J. Geophys. Res.*, **87**, 4585-4594.

Gutenberg, B., and C. F. Richter, 1956: Earthquake magnitude, intensity, energy and acceleration. *Bull. Seismol. Soc. Am.*, 46, 105-145.

Hanks, T. C., 1979: b values and $\omega^{-\gamma}$ seismic source models: implications for tectonic stress variations along active crust fault zones and the estimation of high-frequency strong ground motion. *J. Geophys. Res.*, **84**, 2235-2242.

Hanks, T. C., 1982: f_{max}. *Bull. Seismol. Soc. Am.*, **72**, 1867-1880.

Hanks, T. C., and R. K. McGuire, 1981: The character of high-frequency strong ground motion. *Bull. Seismol. Soc. Am.*, **71**, 2071-2095.

Hartzell, S. H. 1978: Earthquake aftershocks as Green's function. *Geophy. Res. Lett.*, **5**, 1-4.

Hartzell, S. H., and J. Brune, 1979: The Horse Canyon earthquake of August 2, 1975-Two-stage stress release process in a strike-slip earthquake. *Bull. Seismol. Soc. Am.*, 69, 1161-1173.

Haskell, N. A., 1964: Total energy and energy spectral density of elastic wave radiation from propagating faults. *Bull. Seismol. Soc. Am.*, 54, 1181-1841.

Houston, H., and H. Kanamori, 1986: Source characteristics of the Michoacan, Mexico, earthquake at periods of 1 to 30 seconds. *Geophy. Res. Lett.*, **13**, 597-600.

Huang, B. S., K. C. Chen, and Y. T. Yeh, 1996: Source parameters of the December 15, 1993 Tapu earthquake from first P-motions and waveforms. *J. Geol. Soc. China*, **39**, 235-250.

Huang, W. G., and Y. T. Yeh, 1998: The Tapu earthquake of 1993-A study of source parameters using near-source ground motion, *J. Gelo. Soc. China*, **41**, 253-269.

Humphrey, J. R., Jr., and J. G. Anderson, 1994: Seismic source parameters from Guerrero subduction zone. *Bull. Seismol. Soc. Am.*, **84**, 1754-1769.

Kanamori, H., 1994: Mechanics of earthquakes. *Annu. Rev. Earth. Planet. Sci.*, 22, 207-237.

Kanamori, H., and D. L. Anderson, 1975: Theoretical basis of some empirical relations in seismology. *Bull. Seismol. Soc. Am.*, **65**, 1073-1095.

Keilis-Borok, V. I., 1959: On the estimation of the displacement in an earthquake source and of source dimension. *Ann. Geofis.*, **12**, 205-214.

Koyama, J., 1983: Short-period body waves excitations from coherent and incoherent rupture on a fault. *Zisin, Ser. 2*, **36**, 225-235.

Madariaga, R., 1976: Dynamics of an expanding circular fault. *Bull. Seismol. Soc. Am.*, 66, 639-666.

Masuda, T., and Horiuchi, S. and Takagi, A., 1977: Far-field seismic radiation and its depen-

dence upon the dynamic fracture process. *Sci. Rep. Tohoku Univ.*, Ser, **24**, 73-87.

Mogi, K., 1967: Earthquake and fractures. *Tectonophysics*, **5**, 35-55.

Molnar, P., B. T. Tucker, and J. N. Brune, 1973: Corner frequencies of P and S waves and models of earthquake sources. *Bull. Seismol. Soc. Am.*, **63**, 2091-2104.

Ou, G. B., and S. F. Tsai, 1993: The estimation of ground motion in southwestern Taiwan: A study of $M_L - M_W$ relation. *Nat'l Science Council Rep.*, Taiwan, 57pp (in Chinese).

Ou, G. B., and S. J. Tsai, 1995: Determination of the effects of seismic source, anelastic attenuation and site response from observed ground motions records. *Nat'l Science Council Rep.*, Taiwan, 73pp (in Chinese).

Papageorgiou, A. S., K. Aki, 1983: A specific barrier model for the quantitative description of inhomogeneous faulting and the prediction of strong ground motion. I. Description of the model. *Bull. Seismol. Soc. Am.*, **73**, 693-722.

Papageorgiou, A. S., 1988: On two characteristic frequencies of acceleration spectral: patch corner frequency and f_{max}. *Bull. Seismol. Soc. Am.*, **78**, 509-529.

Prucaru, G., and H. Berkhemer, 1982: Quantitative relations of seismic source parameters and a classification of earthquakes. *Tectonophysics*, **84**, 57-128.

Sato, R., and T. Hirasawa, 1973: Body wave spectra from propagation shear crack. *J. Phys. Earth*, **21**, 415-431.

Savage, J. C., 1972: Relation of corner frequency to fault dimensions. *J. Geophys. Res.*, **77**, 3788-3795.

Shin, T. C., C. H. Chang, and C. H. Ching, 1994: The March 1991 Chiali earthquakes sequence. *Meteor. Bull.*, 40, 17-36.

Shin, T. C., 1995: Application of waveform modeling to determine focal mechanisms of the 1993 Tapu earthquake and its aftershocks. *TAO*, **6**, 167-179.

Shin, T. C., W. J. Su, and P. L. Leu, 1987: Coda-*Q* estimates for Taiwan area. *Bull. Geophys.*, *NCU*, **27/28**, 111-118.

Singh, S. K., E. Mena, R. Kind, and F. Kruger, 1987: Evidence for anomalous body wave radiation between 0.4 and 1 Hz from 19 September 1985 Michioacan, Mexico earthquake. Union Geofiscia Mexicana meeting, Ensenada, Nov. 1987.

Takemura, M., T. Ikeura, and T. Uetake, 1993: Characters of source spectra of moderate earthquakes in a subduction zone along the Pacific coast of the Southern Tohoku District, Japan. *J. Phys. Earth*, **41**, 1-19.

Tsai, C. C., 1997: Relationships of seismic source scaling in the Taiwan region. *TAO*, **8**, 49-68.

Wald, D. J., K. Kanamori, D. V. Helmberger, and T. H. Heaton, 1993: Source study of the 1906 San Francisco earthquake. *Bull. Seismol. Soc. Am.*, **83**, 981-1019.

Wang, C. Y., 1988: Calculation of the Q_s and Q_p using the spectral ratio method in the Taiwan area. *Proc. Geol. Soc. China*, **31**, 81-89.

Wang, J, H., 1993: *Q* values of Taiwan: A review. *J. Geol. Soc. China*, **36**, 15-24.

Wang, J. H., and K. S. Liu, 1990: Azimuthal variation of coda *Q* in northern Taiwan. *Geophys. Res. Lett.*, **17**, 1315-1318.

Wang, J. H., T. L. Teng, and K. F. Ma, 1989: Temporal variation of coda Q during Hualien earthquake of 1986 in eastern Taiwan. *PAGEOPH*, **130**, 617-643.

Wang, H. M., 1988: The software design of strong motion data processing. Master's Thesis, Institute of Oceanography, Nat'l Taiwan Univ., Taipei, Taiwan, 81pp (in Chinese).

Yeh, Y. H., and Y. B. Tsai, 1981: Crustal structure of central Taiwan from inversion of P-wave arrival times. *Bull. Inst. of Earth Sciences, Academia Sinica*, **1**, 83-102.

Yeh, Y. H., G. B. Ou, M. H. Tsai, and Y. C. Lin, 1992: The strong-motion observation network in the Chia-Yi and Tai-Nan area. *Nat'l Science Council Rep.*, Taiwan, 81pp (in Chinese).